Accepted Manuscript

Targeting RNA polymerase I transcription machinery in cancer cells by a novel monofunctional platinum-based agent

Zhen-Lei Zhang, Chun-Lai Zhao, Qian Chen, Kai Xu, Xin Qiao, Jing-Yuan Xu

PII: S0223-5234(18)30458-6

DOI: 10.1016/j.ejmech.2018.05.045

Reference: EJMECH 10456

To appear in: *European Journal of Medicinal Chemistry*

Received Date: 16 March 2018

Revised Date: 3 May 2018

Accepted Date: 28 May 2018

Please cite this article as: Z.-L. Zhang, C.-L. Zhao, Q. Chen, K. Xu, X. Qiao, J.-Y. Xu, Targeting RNA polymerase I transcription machinery in cancer cells by a novel monofunctional platinum-based agent, *European Journal of Medicinal Chemistry* (2018), doi: 10.1016/j.ejmech.2018.05.045.

Graphical abstract

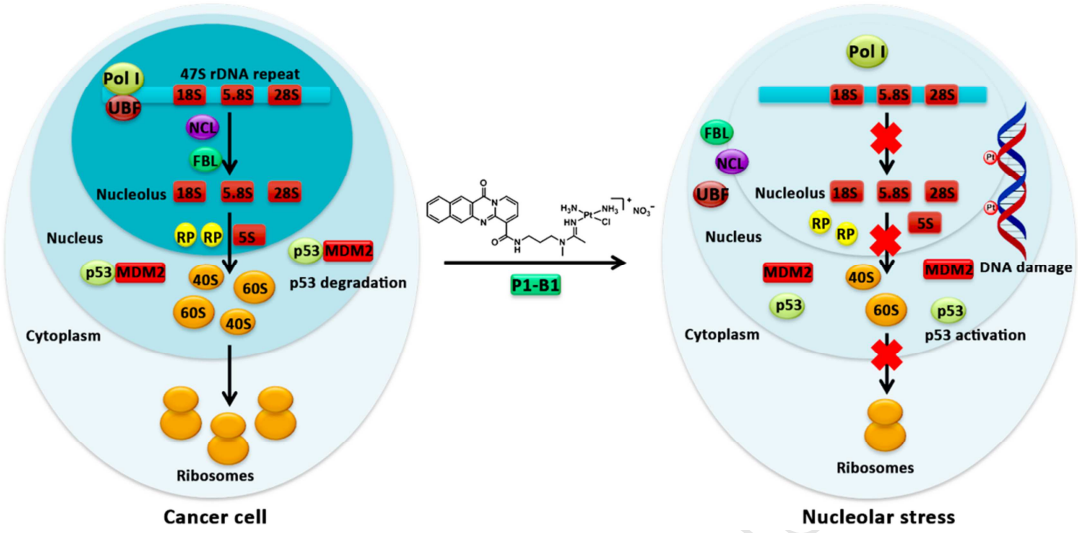

A novel monofunctional platinum-based RNA polymerase I selective inhibitor, **P1-B1**, displays significant nucleolar accumulation, selectively inhibits Pol I transcription, and induces p53 activation as well as nucleolar stress.

Targeting RNA polymerase I transcription machinery in cancer cells by a novel monofunctional platinum-based agent

Zhen-Lei Zhang[‡], Chun-Lai Zhao[‡], Qian Chen, Kai Xu, Xin Qiao[*] and Jing-Yuan Xu[*]

Department of Chemical Biology and Tianjin Key Laboratory on Technologies Enabling Development of Clinical Therapeutics and Diagnostics, School of Pharmacy, Tianjin Medical University, Tianjin 300070, P.R. China.

*Corresponding authors:

J.-Y. Xu: Tel: +86-22-83336929; E-mail: xujingyuan@tmu.edu.cn.

X. Qiao: Tel: +86-22-83336658; E-mail: qiaoxin@tmu.edu.cn

‡ These authors contributed equally.

Abstract

Aberrant ribosome biogenesis and enlarged nucleoli have long been used by pathologists as a marker of aggressive tumors. Suppression of RNA polymerase I (Pol I) transcription machinery within the nucleolus could be a direct way to trigger the nucleolar stress and to inhibit the rapid proliferation of cancer cells. Here we modified cisplatin with an analogue of the RNA polymerase I selective inhibitor BMH-21 to develop a novel platinum-based Pol I selective inhibitor. We show that this novel monofunctional platinum-based agent, **P1-B1**, had enhanced antitumor activity of up to 17-fold greater than the clinical drug cisplatin in cisplatin-resistant non-small cell lung cancer cells. **P1-B1** also had significantly lower cytotoxicity compared than cisplatin as well as the Pol I selective inhibitor BMH-21 in MRC-5 normal lung fibroblast cells, and the selectivity index (SI) greatly increases. Mechanistic investigations revealed that **P1-B1** displayed significant nucleolar accumulation, selectively inhibited Pol I transcription, and induced nucleolar stress, leading to S-phase arrest and apoptosis. Our results suggest that the effects of **P1-B1** are mechanistically distinct from those of conventional platinum agents and the recently described non-classical platinum compounds and that functionalizing platinum-based agents with directly Pol I transcription inhibition properties may represent an improved modality for cancer treatment.

Keywords: Platinum-based anticancer agent; RNA polymerase I transcription machinery; Nucleolar stress; Apoptosis.

1. Introduction

Systemic toxicity and drug resistance are the major limitations for cancer treatment. Platinum-based drugs, for example, have been widely used alone or in combination for nearly 50% of all cancers. However, the clinical use of platinum drugs and other DNA-targeted cytotoxics is compromised by the above shortcomings [1, 2]. On the other hand, cancer cells are highly adaptive and heterogeneous, and the development of robust cell survival circuitries and the inactivation of cell death signaling pathways often lead to chemoresistance [3]. Thus, targeting alternative cellular machineries that are required for proliferation of cancer cells and tumor growth may overcome the drawbacks of conventional anticancer drugs and provide an opportunity for cancer-cell-specific therapy [4].

In mammalian cells, the RNA polymerase I (Pol I) transcription machinery is involved in more than 60% of the total cellular transcriptional activity [5-7]. Cancer cells show increased metabolic activity and a high demand for ribosome biogenesis to support uncontrolled cell proliferation and to manage the stress burden during malignant transformation. Inactivation of tumor suppressors, activation of oncogenes, and up-regulation of protein kinases in cancer cells can promote Pol I transcription and drive cell proliferation [6, 8, 9]. Thus the Pol I transcriptional machinery is the key convergence point for cellular signaling cascades and ribosome production [5]. Indeed, hyperactivated rDNA transcription is consistently elevated in cancer cells. Enlarged nucleoli (hypertrophy), which reflect increased Pol I transcription and ribosome biogenesis, have long been used by pathologists as a marker of aggressive tumors [5]. It appears cancer cells are “addicted” to accelerated ribosome biogenesis and therefore selectively vulnerable to Pol I transcriptional inhibition [2, 7].

Given that aberrant ribosome biogenesis is a hallmark of cancer, disruption of Pol I transcription machinery within nucleolus can be considered a direct way of reactivating the nucleolar stress response and inhibiting the rapid proliferation of cancer cells. Some new inhibitors have been reported for their ability to selectively inhibit rDNA transcription and kill tumor cells [10], such as CX-5461 [8, 11, 12],

CX-3543 [13] and BMH-21 (Scheme 1) [14-16]. The potential of Pol I inhibition has already been realized and resulted in clinical trials, but there is much room for the development of novel Pol I inhibitors.

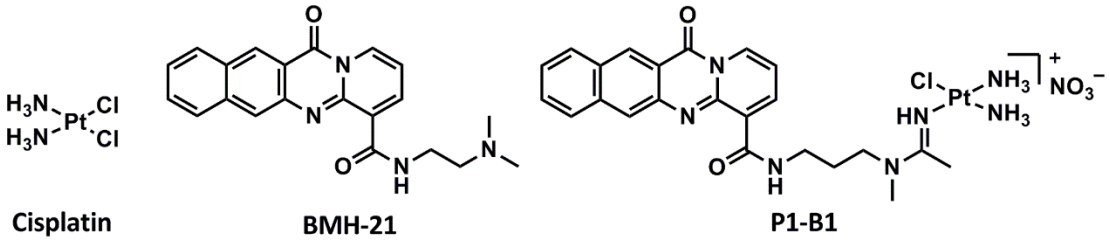

Scheme 1. Structures of cisplatin, BMH-21 and **P1-B1**.

Inspired by the success of current Pol I-selective inhibitors in clinical applications for cancer treatment, we propose that inhibition of Pol I-mediated transcription might be a strategy to overcome the drawbacks of platinum-based therapies. Nucleoli for Pol I transcription are non-membrane-bound sub-nuclear structures with extremely high anionic density, and cationic compounds and cationic metal complexes are therefore able to concentrate in nucleoli, due to electrostatic forces and coordination effects [17-21]. Strikingly, the tandem repeats of rDNA genes are GC rich and nucleosome-free, which renders this form of DNA susceptible to damage by electrophilic agents such as platinum agents and alkylators [2]. A number of studies have shown that rDNA is considered a highly fragile genomic entity, however, the DNA repair machinery, such as transcription-coupled nucleotide excision repair (TC-NER), is not active in rDNA loci [22]. Indeed, multiple platinum-based agents have been reported to act through inhibition of rRNA synthesis [23-25], but none of them are known to selectively target the Pol I transcription machinery. Therefore, construction of platinum-based agents that directly disrupt Pol I transcription is a conceptually attractive strategy.

Until now, no examples of a platinum agent directly targeting RNA Pol I machinery have been reported. Given the aforementioned distinctions between cancer cells and normal tissue, and taking advantage of the potential synergy between Pt

drugs and Pol I selective inhibitors, we employed the Pol I inhibitor BMH-21 analogue (**B1**, Scheme 2) to modify platinum agent, affording a monofunctional platinum Pol I selective inhibitor (**P1-B1**, Scheme 1), with the ability to enhance cytotoxicity in ciplatin-resistant cancer cells and reduce toxicity in MRC-5 normal lung fibroblast cells. Mechanistic studies suggest that the novel monofunctional platinum-based Pol I inhibitor displays significant nucleolar accumulation, selectively inhibits Pol I transcription, which is mechanistically distinct from the effects of classical platinum agents and the recently described non-classical platinum compounds.

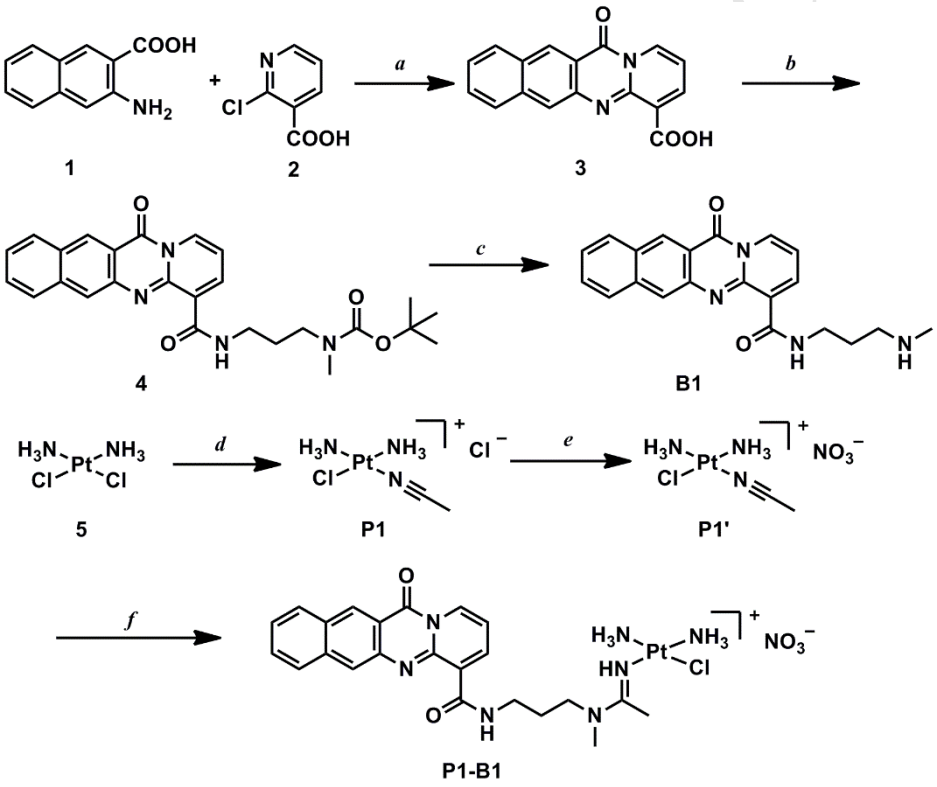

Scheme 2. Synthetic routes for **P1-B1**. Reagents and conditions: *a*. HCl, EtOH; *b*. *tert*-butyl (3-aminopropyl)carbamate, TBTU, DMF, r.t., 24 h; *c*. DCM/TFA, 4 h; *d*. CH_3CN, HCl (pH 4), 70 °C, 2 h; *e*. $AgNO_3$, DMF; *f*. **B1**, DMF, −10 °C, 5 d.

2. Results and discussion

To retain the key structural elements of BMH-21 for Pol I inhibition [26], minor

structural modifications were carried out, affording the BMH-21 analogue **B1** containing secondary amino group for next amidination addition (Scheme 2). Monofunctional platinum-based Pol I inhibitor **P1-B1** was subsequently obtained by amidination reaction of **B1** with platinum precursor derived from cisplatin. The final compound was purified and then characterized by ^{1}H and ^{13}C NMR spectroscopy, and ESI-MS (Fig. S1–S11).

The cytotoxicity of the compounds at 72 h was subsequently evaluated by the MTT assay. Human cancer cell lines including A549 (lung), NCI-H460 (lung), MCF-7 (breast), normal human lung fibroblast MRC-5, as well as cisplatin-resistant cells A549cisR and NCI-H460cisR, were selected to evaluate the *in vitro* anticancer activity of the compounds (Table 1). BMH-21 showed low micromolar or submicromolar toxicity against various human cancer cells, while **B1** and cisplatin displayed micromolar toxicity. However, all these compounds were also very toxic to normal lung fibroblast MRC-5 cells. In different types of cisplatin-sensitive cancer cells, the monofunctional platinum agent **P1-B1** showed up to 9.27-fold increased cytotoxicity compared with cisplatin. More intriguingly, **P1-B1** displayed significant activity in cisplatin-resistant A549cisR and NCI-H460cisR cells, with up to 17.8-fold increase compared with cisplatin. For example, the IC_{50} values of cisplatin in A549 and A549cisR cells are 7.49 and 29.52 μM, respectively, whereas those of **P1-B1** in the same cell lines are 5.42 and 1.66 μM, respectively. The resistance factor (RF), defined as the ratio of the IC_{50} value in cisplatin-resistant cells to that in cisplatin-sensitive cells, is 3.94 for cisplatin, and the RF dramatically decreased to 0.31 for **P1-B1**. The significantly increased cytotoxicity and decreased RF were also observed in NCI-H460 and NCI-H460cisR cells, indicating that amidination of Pol I selective inhibitor moiety with the platinum pharmacophore could effectively overcome the platinum drug resistance. Unexpectedly, **P1-B1** has significantly lower cytotoxicity than cisplatin, **B1**, and BMH-21 in MRC-5 normal lung fibroblast cells, and the selectivity index (SI) greatly increases (Table 1). This emphasizes the important contribution of Pol selective inhibitor towards the selectivity of platinum

agents.

Table 1. Summary of cytotoxicity data for RNA polymerase I inhibitors and Pt compounds (IC_{50} values)[a].

Cell line	CDDP	BMH-21	**B1**	**P1-B1**
A549	7.49 ± 0.70	1.02 ± 0.12	4.34 ± 0.17	5.42 ± 0.48
A549cisR	29.52 ± 1.33	N.D.[b]	N.D.	1.66 ± 0.20
RF[c]	3.94	N.D.	N.D.	0.31
NCI-H460	4.75 ± 1.10	0.20 ± 0.03	1.65 ± 0.09	1.84 ± 0.10
NCI-H460cisR	14.02 ± 0.21	N.D.	N.D.	3.22 ± 1.37
RF	2.95	N.D.	N.D.	1.75
MCF-7	8.63 ± 1.39	0.34 ± 0.01	1.41 ± 0.09	0.93 ± 0.30
MRC-5	2.39 ± 0.30	0.86 ± 0.26	2.42 ± 0.13	16.46 ± 1.70
SI[d] (MRC-5/ A549)	0.32	0.84	0.56	3.04
SI (MRC-5/ MCF-7)	0.28	2.53	1.72	17.70

[a]IC_{50} values ± SD (μM) were extracted from dose-response curves for two experiments performed in triplicate for each concentration. Cells were incubated for 72 h. [b]N.D., not determined. [c]RF (resistant factor) is defined as IC_{50} in A549cisR/IC_{50} in A549 or IC_{50} in NCI-H460cisR/IC_{50} in NCI-H460. [d]SI (selectivity index) is defined as IC_{50} in MRC-5/IC_{50} in A549 or IC_{50} in MRC-5/IC_{50} in MCF-7.

Mechanistic investigations were carried out to study the possible reasons why **P1-B1** expresses increased cytotoxicity compared with cisplatin. The Pol I inhibition activity of BMH-21 has been considered as a result of its selective DNA intercalation. The ehthidium bromide (EB) fluorescence displacement assay by using calf-thymus DNA (CT-DNA) was carried out to clarify the mode of DNA interaction with the synthesized compounds (see supporting information). The emission spectra of EB-DNA system in the absence and presence of the compounds are shown in Fig. S12. The apparent binding constants (K_{app}) at room temperature were calculated to a 10^6

magnitude (Table S1), which were less than ethidium bromide (10^7), indicating that the interactions of the three tetracyclic compounds with DNA are in a moderate intercalative mode. BMH-21 with the strongest K_{app} value has been reported to intercalate with acidic DNA complemented with additional electrostatic interactions [14, 16]. The *N, N'*-dimethylamino group in BMH-21 plays an important role for its potential interaction with the phosphate of DNA backbone [14, 16].The BMH-21 analogue **B1** containing three-carbon link to the carboxamide arm and a basic secondary amino group showed less affinity to CT-DNA, which might attribute to increased linker length and reduced basic charge [14]. By contrast, **P1-B1** showed higher DNA affinity compared with its precursor **B1** as well as the mixture of **B1** and cisplatin. A plausible explanation for this increased DNA affinity would be that **P1-B1**, like other reported monofunctional platinum hybrid agents, such as the acridine- and benz[*c*]acridine-based Pt agents, can interact with DNA through a covalent-intercalative mode and produce hybrid DNA adducts [27-31]. The cationic charge and the covalent binding to adjacent nucleobases produced by **P1-B1** may play key roles for its increases of DNA affinity, which are distinct from the DNA interaction mode of the parent compound BMH-21. This unique DNA binding mode led us to hypothesize that equip platinum agents with Pol I-selective moieties may allow nucleolus-directed DNA binding and induce rDNA damaging [2].

We then tested if the cytotoxic responses produced by **P1-B1** and cisplatin in MCF-7 cells correlate with the intracellular platinum content. Cellular accumulation studies were carried out to determine the distribution of platinum species in whole cells as well as in the nucleoli. A well-defined number of MCF-7 cells were incubated with 10 μM **P1-B1** or cisplatin for 6 h, and the whole-cell samples were lyophilized for platinum content determination. The platinum levels in whole-cell samples were measured by quadrupole inductively-coupled plasma mass spectrometry (ICP-MS). **P1-B1** showed approximately 8.3-fold greater cellular accumulation than cisplatin (Fig. 1). These data demonstrated that the conjugation of pyridoquinazoline moiety with platinum agent resulted in an increased cellular uptake, which may also account

for its higher cytotoxicity in MCF-7 cells compared with cisplatin. By contrast, cisplatin accumulates in MCF-7 cells at a slower rate than **P1-B1**, which leads to significantly lower levels of intracellular platinum content. This can be expected based on the charge status of the two agents. Cisplatin as well as other classical platinum agents are electroneutral compounds, and passive diffusion is a major cell uptake pathway for cisplatin-type compounds [32-34]. Clearly, **P1-B1** is a cationic monofunctional platinum compound, in which accumulation of positive charge facilitate cellular uptake [34].

To further investigate the intracellular distribution of the pyridoquinazoline compounds as well as **P1-B1**, we used confocal fluorescence microscopy by taking advantage of the intrinsic green fluorescence of the pyridoquinazoline moiety. MCF-7 cells were dosed with BMH-21, **B1**, and **P1-B1** at 10 μM for 4 hours. Treated cells were then fixed by 4% paraformaldehyde in PBS and observed under confocal fluorescence microscopy (see the supporting information). The nuclei and nucleoli of MCF-7 cells could be readily identified in the merged and bright field images without nuclear staining. The fluorescence spectra of the three pyridoquinazoline compounds in PBS (10 μM, λ_{ex} = 450 nm) showed that the fluorescent intensity of BMH-21 was weaker than the other two compounds in the same condition (Fig. S13). However, the intracellular fluorescence intensity in green channel observed for BMH-21 in MCF-7 cells showed significantly higher than for **B1** and **P1-B1**, suggesting a higher cellular uptake and a better cytotoxicity of BMH-21 in various cancer cells (Fig. S14). BMH-21 produced significant green fluorescence in the nuclei but less green fluorescence in the cytosol, which is consistent with its DNA intercalating property and high cytotoxicity [14, 16]. By contrast, the fluorescence intensities observed for **B1** and **P1-B1** were lower than for BMH-21 in the nucleus, but both **B1** and **P1-B1** showed a high degree of distribution within nucleolus, suggesting major differences in subcellular levels of these three structurally related heteroaromatic compounds. **P1-B1** showed weaker intracellular fluorescence intensity compared with **B1**, which suggests that increasing molecule weight might slightly perturb the cell entry process of the

tetracyclic compounds and lead to decrease in cell uptake as well as toxicity. Nevertheless, the results imply that functionalize platinum-based agents with directly Pol I transcription inhibitor may increase platinum nucleolar accumulation and produce rDNA damage as well as selective cell killing.

We also studied the Pt levels in nucleoli of MCF-7 cells. The nucleoli were extracted and identified according to well-established protocol and the platinum content was determined by ICP-MS (Fig. 1). Nucleoli extracted from well-defined number of MCF-7 cells dosed with **P1-B1** displayed significantly high levels of platinum (17 ng Pt/10^6 cells, approximately 5.3% of that detected for whole-cell samples). Using a combination of electron microscopy and X-ray probe microanalysis, Khan and Sadler have observed Pt accumulation in the nucleolus and on the inner edge of nuclear membrane after 4 hour treatment with 200 μM cisplatin [35]. However, under the specific conditions of this experiment, the nucleolar platinum levels in cisplatin treated cells were below the limits of detection. Again, as a cationic platinum compound, **P1-B1** has a high intrinsic affinity for the negatively charged biopolymer and the subcellular compartments with extremely high anionic density, such as nucleoli. Unlike cisplatin, **P1-B1** does not require aquation steps to produce a cationic form to promote electrostatic association, and the cationic nature of **P1-B1** can be considered one driving force that enhances the nucleolar targeting of this agent [24, 34]. On the other hand, preferential binding of pyridoquinazoline moiety to GC-rich sequences [16, 26], especially to highly GC-rich rDNA, can play a decisive role for the nucleolar accumulation of **P1-B1**. Given that rDNA is highly fragile gemomic entity and lack effective transcription-coupled nucleotide excision DNA repair machinery [22], the rapid and selective nucleolar platinum accumulation can consequently lead to selective Pol I inhibition and trigger nucleolar stress and apoptosis.

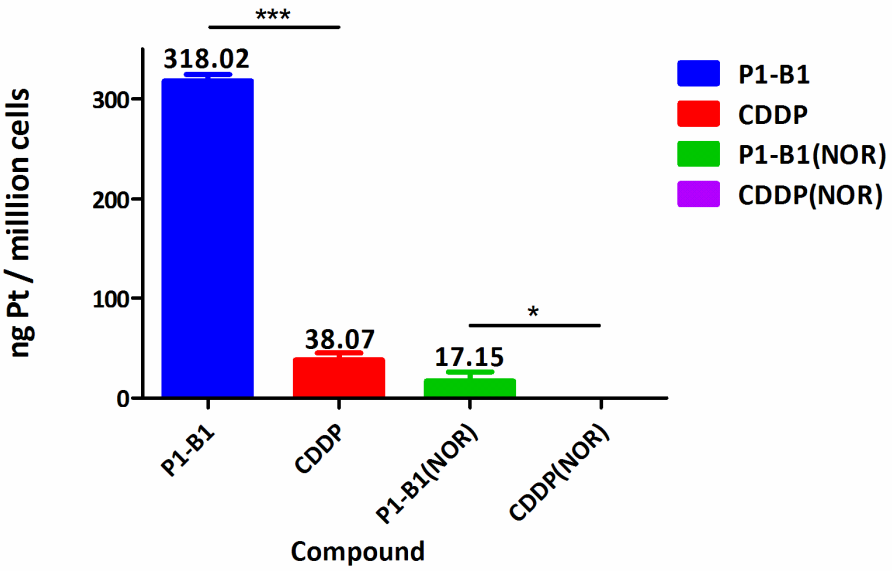

Fig. 1. Cellular and nucleolar (NOR) platinum content in MCF-7 cells treated with 10 μM cisplatin or **P1-B1** for 6 h. The data are presented as the mean ± standard deviation of three independent experiments. Results are expressed as the mean ± standard deviation (S.D.) (n = 3). *P < 0.05; ***P < 0.001 compared with the control group.

To assess whether **P1-B1** affects Pol I transcription machinery, we first analyzed *de novo* RNA synthesis using 5-ethynyluridine (EU) incorporation. MCF-7 cells were treated with different compounds (10 μM) for 4 h, and newly synthesized RNA was labeled by Alexa Fluor 647 azide using orthogonal click reaction (Fig. 2, Fig. S15). Using confocal microscopy, we observed that Alexa Fluor 647 (red) fluorescence is confined to the nucleus of untreated MCF-7 cells and shows the highest intensity in the nucleolus, consistent with the high rate of rRNA synthesis for ribosomal biogenesis. By contrast, cells exposed to compounds showed significantly decreased EU incorporation. Strikingly, unlike higher red fluorescence in the nucleolar region with cisplatin incubation, **P1-B1** results in a dramatic decrease within the nucleolar region (Fig. 2). This observation supports that the nucleolar accumulation of **P1-B1** has a major effect on Pol I mediated rRNA synthesis. It has been proposed that

perturbing Pol II by Pt-DNA adducts plays an important role for traditional bifunctional crosslinking platinum agents [25, 30]. Therefore, inhibition of Pol II transcription machinery in the nucleoplasm was an expected outcome for cisplatin. In addition, the selective loss of EU incorporation in nucleolus observed after treatment with **P1-B1** suggests a potential mechanism would involve accumulation of platinum into the nucleoli and inhibition of the Pol I transcription machinery by adducts generated in rDNA.

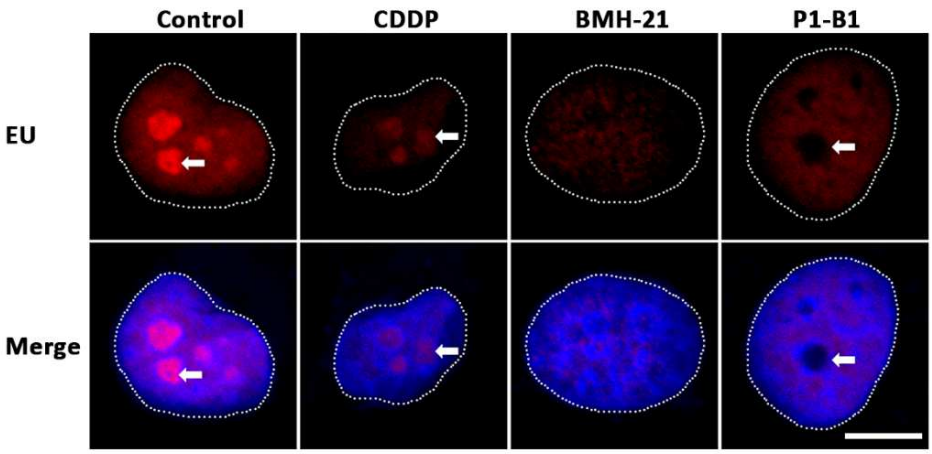

Fig. 2. Representative images of EU incorporation (1 h) in MCF-7 cells after 4 h treatment with 10 μM cisplatin, BMH-21 or **P1-B1**. Cells were co-stained with DAPI nuclear dye. The white arrows highlight nucleolar regions before and after treatment. Scale bars represent a length of 10 μm. (For additional views of EU incorporation images, see the electronic supplementary material Fig. S15)

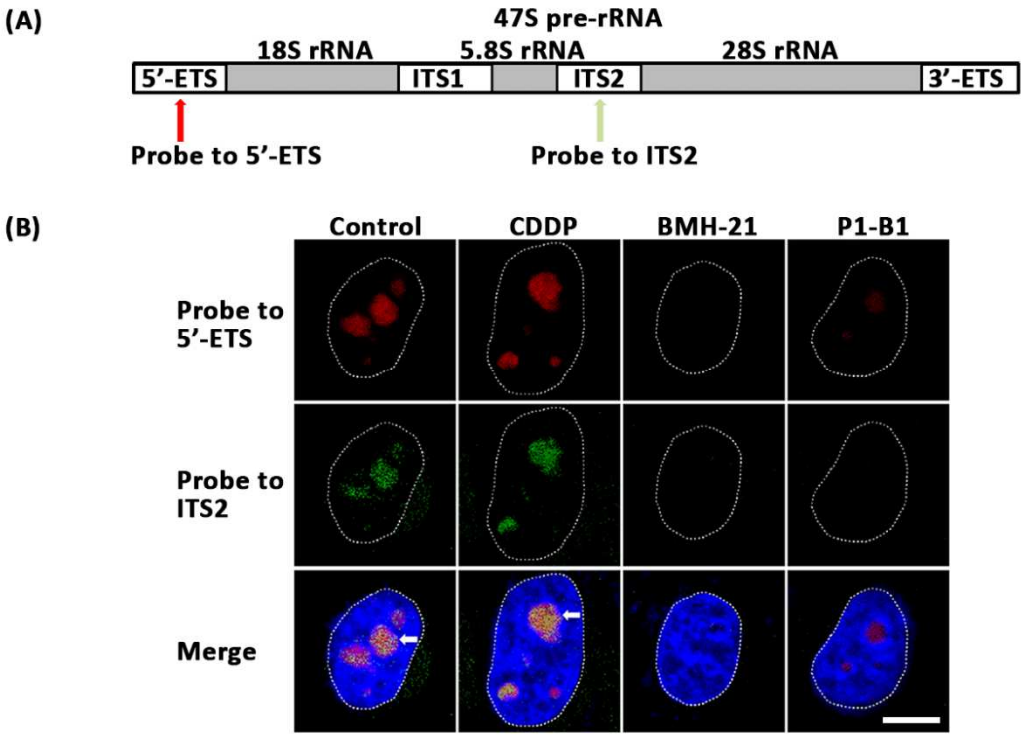

Fig. 3. Fluorescent *in situ* hybridization (FISH) to observe the disruption of 47S pre-rRNA. (A) Cy5-labeled probe for 5'-ETS (red) and Cy3-labled probe for ITS2 (green). (B) MCF-7 cells, untreated or treated for 3 h with 10 μM cisplatin, BMH-21, or **P1-B1**, were washed, fixed, and analyzed by FISH using Cy5-labeled probe for 5'-ETS (red) and Cy3-labled probe for ITS2 (green). Cellular nuclei were stained with DAPI (blue). The white arrows highlight nucleolar regions. Scale bars represent a length of 10 μm. (For additional views of FISH images, see the electronic supplementary material Fig. S16)

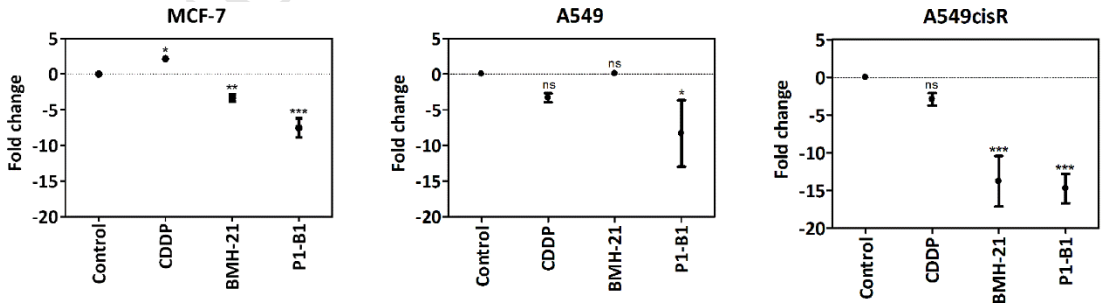

Fig. 4. 45S pre-rRNA expression levels in MCF-7, A549 or A549cisR cells after 3 h treatment with 10 μM cisplatin, BMH-21 or **P1-B1**. MCF-7, A549 and A549cisR cells,

untreated or treated with 10 μM cisplatin, BMH-21, **B1** or **P1-B1** for 3 h, and the total RNA was harvested for quantitative real-time polymerase chain reaction (qRT-PCR). Results are expressed as the mean ± standard deviation (S.D.) (n = 3). **P* < 0.05; ****P* < 0.001; ns, non-significant difference compared with the control group.

To further confirm the Pol I inhibition effects, we next analyzed the impact of **P1-B1** on Pol I transcription by fluorescent *in situ* hybridization (FISH) for the 47S rDNA repeats, using probes that hybridize to external transcribed spacer 5'-ETS (labeled by Cy5, red) or internal transcribed spacer ITS2 (labeled by Cy3, green). Confocal images were taken of untreated cells and compound-treated cells after hybridization. Three-hour treatment of MCF-7 cells with 10 μM **P1-B1** was accompanied by a dramatic condensation of the 5'-ETS rDNA within the nucleoli to punctate foci and a marked decrease in red Cy5 fluorescence relative to untreated cells or cisplatin-treated cells, which is characteristic of a reduced Pol I transcription rate. Interestingly, just like BMH-21, a complete depletion of green Cy3 fluorescence for ITS2 rDNA is observed in cells that were treated with 10 μM **P1-B1**, consistent with dramatic loss of 5'-ETS fluorescence intensity (Fig. 3, Fig. S16). This observation suggests that BMH-21 and **P1-B1** share qualitatively similar Pol I selective inhibition patterns. To strengthen these data, we measured the amount of 45S pre-rRNA as a readout for rDNA transcription by qRT-PCR. MCF-7, A549, and A549cisR cells were treated with **P1-B1** (10 μM), and the total RNA was harvested after 3 h for quantitative real-time polymerase chain reaction (qRT-PCR) analysis of 45S pre-rRNA expression (Fig. 4). The results show that 45S pre-rRNA expression levels dramatically decreased by up to 13.7-fold relative to untreated cells. On the contrary, weak decreases of 45S pre-rRNA expression were observed in cisplatin-treated cells. Significant inhibition of cellular 45S pre-rRNA expression further supported its unique ability to interrupt the Pol I transcription machinery, thereby inducing the nucleolar stress pathway.

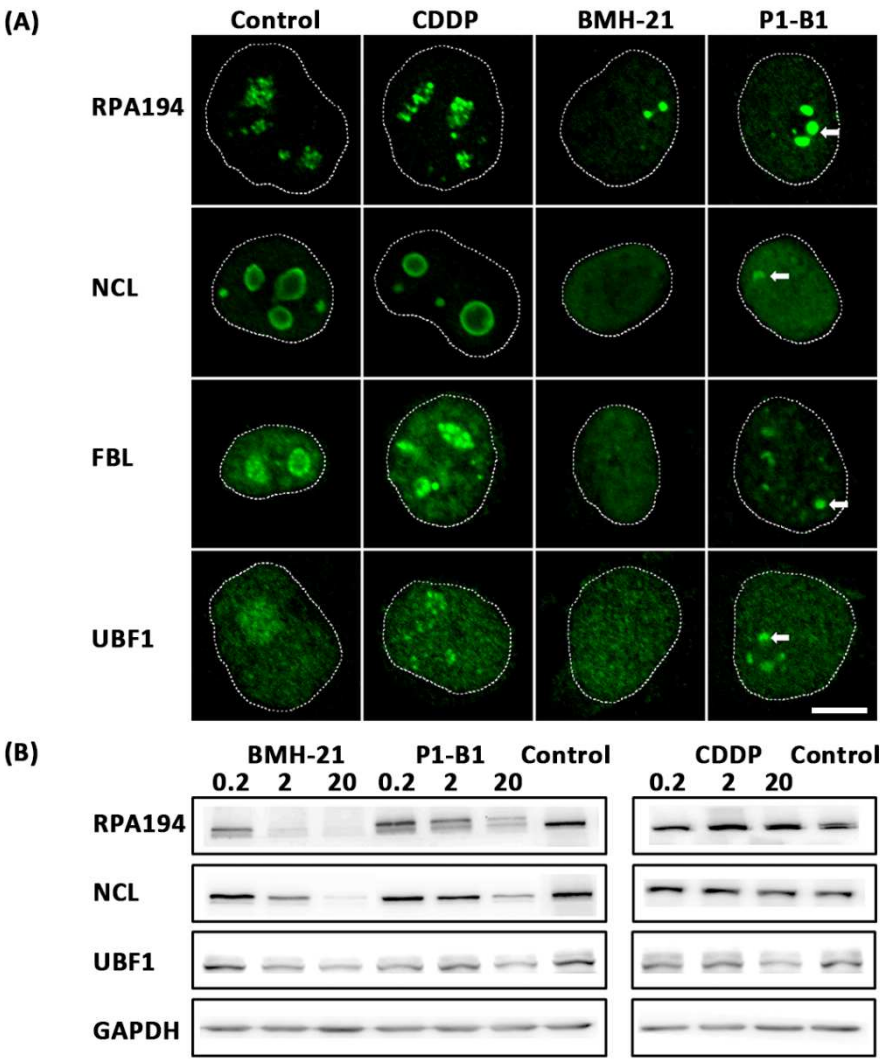

Fig. 5. (A) Representative images of **P1-B1** induced segregation and nucleoplasmic translocation of nucleolar proteins. MCF-7 cells were untreated or treated with 10 μM cisplatin, BMH-21, or **P1-B1** for 4 h and stained for RPA194, NCL, FBL, and UBF1. The white arrows indicate nucleolar caps. Scale bars represent a length of 10 μm. (B) Western blot analysis of RPA194, NCL, and UBF1 in MCF-7 cells. MCF-7 cells were untreated or treated with 10 μM cisplatin, BMH-21, or **P1-B1** for 12 h. Relative expression levels of RPA194, NCL, and UBF1 are presented as the mean ± standard deviation of relative grayscale values from two independent experiments. (For additional views of segregation and nucleoplasmic translocation of nucleolar proteins and comparisons of nucleolar protein expression, see the electronic supplementary material Fig. S17, S18)

Disruption of the nucleolar structure and alterations in nucleolar protein localization and dynamics are a hallmark of Pol I transcription stress [5, 22]. To assess whether **P1-B1** affect the integrity of the nucleolus, we treated MCF-7 cells with **P1-B1** at 10 μM concentration for 4 hours after which the cells were fixed and stained for Pol I catalytic subunit RPA 194, fibrillar center proteins upstream binding factor (UBF) and fibrillarin (FBL), and granular component protein nucleolin (NCL) (Table S2). We observed that **P1-B1** was capable of inducing segregation of UBF, RPA194 and FBL into nucleolar caps, as did BMH-21 (Fig. 5, Fig. S17, S18). Concomitantly, a prominent translocation of NCL from the nucleolus to nucleoplasm was observed in **P1-B1** treated MCF-7 cells. By contrast, cisplatin did not cause disintegration of the nucleolus after 4 h treatment. The unique segregation of the nucleolus and dislocation of nucleolar protein upon **P1-B1** treatment further indicates that **P1-B1** has a mechanism of action that is distinct from cisplatin and more similar to that of BMH-21. We then analyzed the effects of **P1-B1** on expressions of Pol I transcription machinery proteins, including UBF, RPA194 and NCL. As determined by Western blotting, the expression levels of UBF decreased mildly upon treatment with cisplatin, showing that cisplatin indeed perturbed UBF, which was likely from its crosslinking effect. This is consistent with the previously reported evidence that the crosslinking agent cisplatin affect Pol I transcription by distracting UBF from binding the rDNA and promoting Pol I transcription [36, 37]. In stark contrast, 12 h incubation of **P1-B1** remarkably decreased expressions of RPA194 and NCL in a dose-dependent manner, and to a lesser extent, that of UBF. Collectively, these results suggest that inhibition of rRNA transcription is an imminent response to treatment of **P1-B1**, followed by segregation of the nucleolus, dislocation of nucleolar protein and loss of Pol I catalytic subunit RPA194.

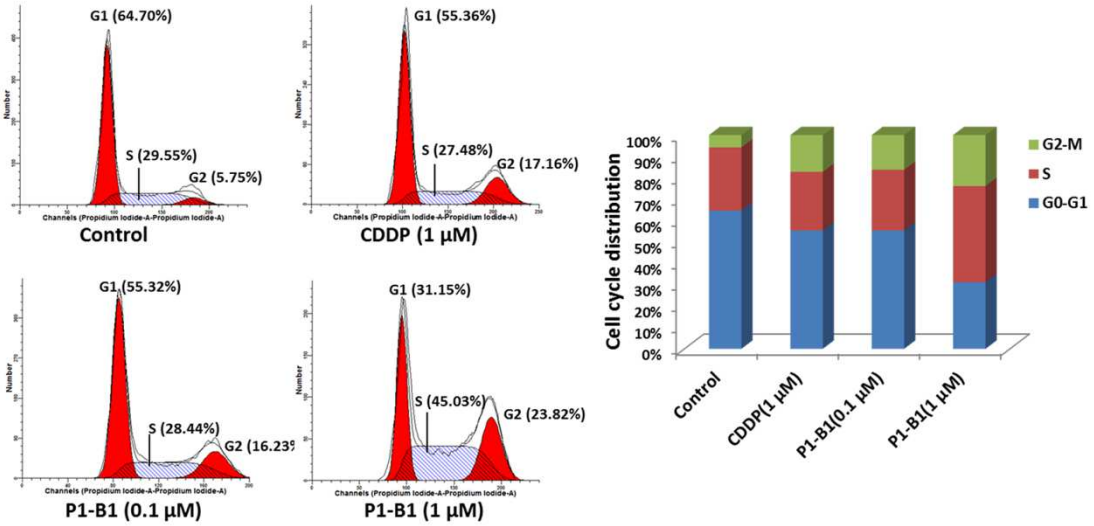

Fig. 6. Effects of platinum compounds on the cell cycle progression in MCF-7 cells. MCF-7 cells, untreated or treated with 0.1, 1 μM cisplatin or **P1-B1** for 48 h, were stained with propidium iodide (PI), and cell cycle distribution was analyzed by flow cytometry.

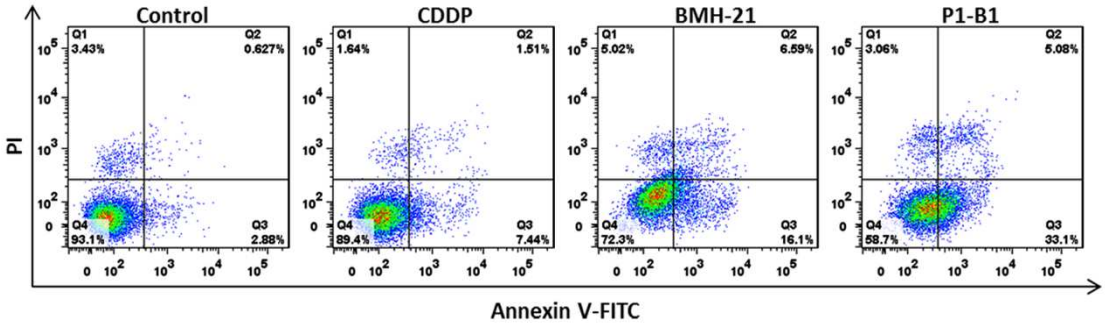

Fig. 7. Apoptosis induced by **P1-B1**. MCF-7 cells, untreated or treated with 1 μM cisplatin, BMH-21 or **P1-B1** for 24 h, then processed for Annexin V/PI double staining and analyzed by flow cytometry. Annexin V-positive/PI-negative cells are in the early stages of apoptosis and double positive cells are in late apoptosis.

Pol I transcriptional inhibition has been demonstrated to lead to nucleolar stress that causes p53 stabilization and apoptosis. We therefore scrutinized whether the **P1-B1** killed cancer cells by activating p53 [38]. After 4 h of incubation, we observed increased p53 green fluorescence in BMH-21 and **P1-B1**, but not in cisplatin-treated cells (Fig. S14). This observation leads us to believe that selective Pol I inhibition and

nucleolar stress produced by **P1-B1** can indeed initiate a rapid increase in p53 stabilization. We then performed flow cytometry analysis to determine the effect of **P1-B1** exposure on cell cycle progression. As shown in the cell cycle distribution, cisplatin arrested the cell cycle at the S phase. Cells treated with 1 μM **P1-B1** displayed larger S-phase populations after 48 h compared with cisplatin, indicative of a strong S-phase arrest (Fig. 6). We also carried out the Annexin V/propidium iodide (PI) dual staining assay to quantify apoptosis induced by **P1-B1** in MCF-7 breast cancer cells. After cells were exposed to **P1-B1** (1 μM) for 24 h, 33% of the cell population displayed characteristics associated with early apoptosis (Fig. 7). These results also implies that the nucleolar stress produce by **P1-B1** is a fast and decisive process for its cell killing, which might be independent of DNA repair machinery and directly trigger cell cycle arrest and apoptosis.

3. Conclusions

In summary, we present a monofunctional platinum-based Pol I selective inhibitor **P1-B1** that preferentially targets the RNA polymerase I transcription machinery to provoke nucleolar stress. **P1-B1** displayed significantly increased cytotoxicity in cisplatin-resistant cells, and the compound was less toxic to normal cells, showing higher efficacy and superior therapeutic index compared with cisplatin. Profound mechanism studies revealed that **P1-B1** effectively entered cancer cells, markedly accumulated into nucleoli, and selectively inhibited Pol I transcription. Our cellular data provide evidence for induction of nucleolar stress, which leads to S-phase arrest and apoptosis. We cannot exclude the possibility that **P1-B1** might have other targets than Pol I transcription machinery. However, the unique pattern of loss nucleolar integrity, together with p53 stabilization and apoptosis, clearly indicated that the selective Pol I inhibition plays a key role in the cytotoxicity of **P1-B1**. Although several organic small molecules [10], such as ellipticines, CX-5461, CX-3543 and BMH-21, have shown selective Pol I inhibition, this would be an unprecedented mechanism of a platinum-based agent. Significantly, we observed that

none of the known platinum agents induced loss of RPA194, suggesting that inhibition of Pol I produced by **P1-B1** is mechanistically distinct from the effects of conventional platinum agents [36, 37, 39] and the recently described non-classical platinum compounds [23-25]. Nevertheless, this study highlights the importance of functionalizing platinum-based agents with directly Pol I transcription machinery inhibition as a cancer-specific strategy for developing novel platinum-based agents. Future work will also address if the chemical modification can used to deliver a dissociable platinum agent to the nucleolus. Additional *in vivo* evaluations of **P1-B1** and further mechanistic studies are currently underway.

4. Experimental section

4.1 Materials and physical measurements

Except where otherwise noted, all the reagents and solvents were bought from commercial suppliers and used as received without further drying or purification. All the reactions were carried out under normal atmospheric conditions with protection from light. Nuclear magnetic resonance (NMR) spectra were measured on Bruker AVANCE III 400 MHz NMR spectrometer. Chemical shifts (δ) are given in parts per million (ppm) relative to internal standard tetramethylsilane (TMS). ^{1}H NMR data is reported in the conventional form including chemical shift (δ, ppm), multiplicity (s = singlet, d = doublet, t = triplet, q = quartet, m = multiplet, br = broad), coupling constants (Hz), and signal integrations. The NMR spectra were processed and analyzed using the MestReNova software package. Electrospray ionization mass spectra (ESI-MS) were obtained on an Agilent API-150EX MS system. Analytical reversed-phase high-performance liquid chromatography (HPLC) was conducted on a Shimadzu Prominence HPLC system using a Venusil XBP C18 column (5 μm, 150 Å, 250 × 4.60 mm, 1 mL·min^{-1} flow). Elemental analyses for C, H and N were obtained on a Perkin-Elmer analyzer model 240. Confocal microscopic images were scanned

by Laser Confocal Scanning Biological Microscope Olympus FV1000.

4.2 Synthesis and Characterization.

4.2.1 12-Oxo-12H-benzo[g]pyrido[2,1-b]quinazoline-4-carboxylic acid (3)

A mixture of 3-amino-2-naphthoic acid (**1**) (4.00 g, 21.36 mmol), 2-chloronicotinic acid (**2**) (3.36 g, 21.36 mmol), and hydrochloric acid (1.8 mL, 60.00 mmol) in ethanol (150 mL) was stirred at 80 °C for 72 h. After cooling, the reddish-orange suspension was filtered, washed with ethanol, and air-dried to afford **3** as a yellow-orange solid [26]. Yield: 2.12 g, 50.4%. ^{1}H NMR (400 MHz, DMSO-d_6) δ ppm 9.15 (s, 1H), 9.00 (dd, *J* = 7.3, 1.4 Hz, 1H), 8.60 (dd, *J* = 6.9, 1.3 Hz, 1H), 8.48 (s, 1H), 8.33 (d, *J* = 8.4 Hz, 1H), 8.18 (d, *J* = 8.4 Hz, 1H), 7.79−7.72 (m, 1H), 7.67−7.60 (m, 1H), 7.16 (t, *J* = 7.1 Hz, 1H).

4.2.2

Tert-butylmethyl(3-(12-oxo-12H-benzo[g]pyrido[2,1-b]quinazoline-4-carboxamido)propyl)carbamate (4)

A mixture of **3** (200 mg, 0.68 mmol), TBTU (332 mg, 1.04 mmol), and DIPEA (360 μL, 2.08 mmol) in DMF (5 mL) was stirred at room temperature for 20 min. Then *tert*-butyl (3-aminopropyl)carbamate (181.2 mg, 1.04 mmol) was added and stirring continued for 24 h. The reaction mixture was added to 100 mL of cold water with stirring. The solid was collected by filtration and dried under vacuum to afford **4** as a yellow solid. Yield: 221 mg, 70.6%.

4.2.3

*N-(3-(methylamino)propyl)-12-oxo-12H-benzo[g]pyrido[2,1-b]quinazoline-4-carboxamide(**B1**)*

To a solution of **4** (221 mg, 0.48 mmol) in dichloromethane (4 mL) was added

TFA to a final concentration of 10% (v/v). The mixture was stirred at room temperature for 4 h and then was washed with a solution of saturated sodium bicarbonate. The layers were separated and the organic layer was dried over sodium sulfate, filtered, concentrated and dried under vacuum to afford crude product. The solids were purified by chromatography using DCM/MeOH/Et_3N (20 : 1 : 0.1) as an eluent. The solvent was then evaporated under vacuum to afford yellow solid **B1**. Yield: 130 mg, 75.2%. ^{1}H NMR (400 MHz, DMSO-d_6) δ 10.89 (t, *J* = 5.5 Hz, 1H), 8.85 (s, 1H), 8.74 (dd, *J* = 7.3, 1.6 Hz, 1H), 8.41 (dd, *J* = 6.9, 1.6 Hz, 1H), 8.14–8.06 (m, 2H), 7.96 (d, *J* = 8.4 Hz, 1H), 7.66–7.57 (m, 1H), 7.52–7.44 (m, 1H), 6.94 (t, *J* = 7.1 Hz, 1H), 3.53–3.43 (m, 2H), 2.67 (t, *J* = 6.9 Hz, 2H), 2.37 (s, 3H), 1.80 (p, *J* = 6.8 Hz, 2H). ^{13}C NMR (101 MHz, DMSO-d_6) δ 161.90, 158.75, 145.20, 140.78, 139.45, 136.64, 130.05, 129.68, 129.26, 128.92, 128.50, 127.20, 125.76, 125.37, 122.78, 115.30, 110.85, 49.34, 37.35, 36.24, 29.04. Elemental analysis (%): calc. for $C_{21}H_{20}N_4O_2$: C, 69.98; H, 5.59; N, 15.55. Found: C, 69.89; H, 5.65; N, 15.48.

*4.2.4 $Pt(NH_3)_2(CNCH_3)Cl_2$ (**P1**)*

$Pt(NH_3)_2Cl_2$ (60 mg, 0.2 mmol) was heated under reflux in 4 mL of dilute HCl (pH 4) with acetonitrile (1.0 mL, 19.2 mmol) until the yellow suspension turned into a colorless solution (about 2 h). Solvent was evaporated under vacuum, and the pale-yellow residue was redissolved in 2 mL of anhydrous MeOH. A small amount of insoluble yellow solid was removed by membrane filtration and the colorless filtrate was added directly into 40 mL of vigorously stirred dry diethyl ether, affording **P1** as an off-white microcrystalline precipitate. Yield: 50 mg, 73.3%. ^{1}H NMR (400 MHz, D_2O) δ ppm 2.55 (s, 3H).

*4.2.5 **P1-B1***

P1 (50 mg, 0.15 mmol) was converted to its nitrate salt by reaction with $AgNO_3$ (25 mg, 0.15 mmol) in 2 mL of anhydrous DMF. AgCl was removed by syringe filtration, and the filtrate was cooled to −10 °C. **B1** (60 mg, 0.17 mmol) was added to

the solution, and the solution was stirred at −10 °C for 5 days [29]. The mixture was added into 40 mL of diethyl ether. The yellow slurry was stirred for 24 h, and the precipitate was recovered by membrane filtration and dried in a vacuum overnight. The product was further purified by recrystallization from hot methanol to afford **P1-B1** as a microcrystalline yellow-orange solid. Yield: 70 mg, 64.1%. HPLC analytical purity: 97.5%. ^{1}H NMR (400 MHz, DMSO-d_6) δ ppm 10.99–10.89 (m, 1H), 9.05 (s, 1H), 8.88 (d, *J* = 7.0 Hz, 1H), 8.48 (d, *J* = 6.4 Hz, 1H), 8.39 (s, 1H), 8.26 (d, *J* = 8.0 Hz, 1H), 8.13 (d, *J* = 8.1 Hz, 1H), 7.70 (t, *J* = 7.1 Hz, 1H), 7.58 (t, *J* = 7.1 Hz, 1H), 7.03 (t, *J* = 6.7 Hz, 1H), 5.80 (s, 1H), 4.87–4.50 (m, 1H), 4.19 (s, 2H), 3.91 (s, 2H), 3.57–3.44 (m, 4H), 3.01 (s, 3H), 2.54 (s, 3H), 2.01–1.87 (m, 2H). ^{13}C NMR (101 MHz, DMSO-d_6) δ ppm 165.49, 162.51, 158.90, 145.30, 140.98, 139.42, 136.79, 130.19, 129.85, 129.35, 129.01, 128.59, 127.34, 125.88, 125.63, 123.18, 115.46, 110.93, 40.43, 36.74, 36.57, 22.31. MS (ESI, positive-ion mode): calcd for $C_{23}H_{30}ClN_7O_2Pt$ ($[M+H]^+$), 666.1797; found: 666.1693. Elemental analysis (%): calc. for $C_{23}H_{29}ClN_8O_5Pt$: C, 37.94; H, 4.01; N, 15.39. Found: C, 37.84; H, 4.09; N, 15.30.

4.3 Biological studies

4.3.1 Sample preparation

Stock solutions of BMH-21, **B1** and **P1-B1** were prepared in DMF and concentrations were determined spectrophotometrically by ε_{266} = 47230 $M^{-1}\cdot cm^{-1}$. Cisplatin (CDDP) was purchased from Boyuan Pharmaceutical (Shandong, China). Stock solution of cisplatin was prepared in phosphate-buffered saline (PBS) and the concentration was determined by ε_{300} = 132 $M^{-1}\cdot cm^{-1}$ [40]. For cytotoxicity evaluation, culture media were used to prepare the working solutions of the compounds by 2-fold serial dilution, in which the final percentages of organic solvent DMF were less than 0.5%. For other biological experiments, the DMF concentrations were also much lower than 0.1%.

4.3.2 Cell culture

The human lung carcinoma A549, NCI-H460, breast adenocarcinoma MCF-7 and cervical adenocarcinoma HeLa cells were obtained from American Type Culture Collection (Rockville, MD, USA). The human lung carcinoma A549cisR, NCI-H460cisR and human lung fibroblast MRC-5 were obtained from Peking Union Medical College (National Infrastructure of Cell Line Resource, China). A549, MCF-7 and HeLa cells were maintained in DMEM supported with 10 % fetal bovine serum (FBS) and 100 $U \cdot mL^{-1}$ penicillin/streptomycin. NCI-H460 and NCI-H460cisR cells were maintained in RPMI 1640 medium supported with 10% FBS, 2 mM L-glutamine, and 100 $U \cdot mL^{-1}$ penicillin/streptomycin. A549cisR were maintained in McCoy's 5A medium supported with 10% FBS. MRC-5 were maintained in minimum essential medium (MEM) supported with 10% FBS. For the culturing of A549cisR and NCI-H460cisR cells, 20-40 μM cisplatin was added to the culture medium every two passages. After induction periods of 72 h, cells were rinsed by PBS and incubated in fresh medium for one week. All the cells were incubated in a humidified incubator at 37°C with 5% CO_2.

4.3.3 Cell viability assay

The viability of cancer cells exposed to the compounds was measured by an MTT assay. Cells were seeded in 96-wellplates at a density of 2000 cells/well, after overnight incubation, cells were treated with varying concentrations of testing compound for 72 h at 37 °C in an atmosphere of 5% CO_2. After incubation periods of 72 h, 10 μL of MTT solution was added to each well and incubated at 37 °C for 4 h. The medium was removed and DMSO (100 μL) was added to each well to dissolve the formed purple formazan. The absorbance of formazan was measured at 570 nm using an Infinite 200 Pro NanoQuant Microplate Reader (Tecan, Swiss).

4.3.4 Cellular accumulation of platinum

To determine the intracellular Pt content, exponentially-growing MCF-7 cells (1

× 10^6 per well) were seeded in six-well plates with 2 mL of media and were allowed to attach overnight. Cells were incubated in the presence of 10 μM compounds at 37 °C for 6 h. Incubations were performed in triplicated for each compound. Cells were washed three times with 2 mL of ice-cold PBS to quench the incubations. The cells were then collected by trypsinization and completely removed from the dishes by additional washings with cold PBS. Cell suspensions were centrifuged at 1500 rpm for 5 min. Whole-cell samples were lyophilized using a freeze dry system. The platinum concentration in the lyophilized samples was determined by quadrupole inductively-coupled plasma mass spectrometry (ICP-MS). Prior analysis, lyophilized samples were digested in the presence of 0.2 mL high-purity nitric acid for 4 h at room temperature. Samples were diluted by adding 2 mL deionized water and were centrifuged at 5000 rpm for 15 min. After centrifugation, an aliquot (0.2 mL) of each digested sample was transferred to an ICP-MS autosampler tube for platinum content determination. The Thermo iCAP Q ICP-MS was calibrated with Pt-containing acid matrix. The platinum contents expressed as ng Pt / million cells.

4.3.5 Nucleolar isolation

To determine the nucleolar Pt content, exponentially-growing MCF-7 cells (1 × 10^6 per well) were seeded in six-well plates with 2 mL of media and were allowed to attach overnight. Cells were incubated in the presence of 10 μM platinum compounds at 37 °C for 6 h. Incubations were performed in triplicated for each compound. Just before nucleolar isolation, the culture medium was decanted from the dishes, and a cold Solution I (0.5 M sucrose with 3 mM $MgCl_2$), 1% phenylmethanesulfonyl fluoride (PMSF) was added to quench all metabolic activities. All of the solutions were pre-cooled at −20 °C, the high percentage of sucrose in the solutions prevents them from freezing at this temperature. The solution was quickly decanted, followed by 3 rapid rinses with the same volume of Solution I. After the removal of the last wash, the cells were quickly scraped from the plate on ice into a 1.5 mL tube. Solution I was added into the collected cells to make up a volume of 0.5 mL. To break down

the cells and release the nucleoli, the cells were sonicated on ice at 100 W, 10 seconds on, 10 seconds off, for 5 times. The sonicated cells were checked under a microscope, in order to ensure that more than 90% of the cells were broken. Then, the cell lysate was underlaid with 0.7 mL of Solution II (1.0 M sucrose, 3 mM $MgCl_2$). The tube was centrifuged at 1800 × g for 5 min at 4 °C. The resulting pellet contained isolated nucleoli [41]. The supernatant was carefully removed, so that the sucrose layers were not disturbed. The pellet was transferred to a new tube and lyophilized using a freeze dry system. The platinum concentration in the lyophilized nucleolar samples was determined by ICP-MS.

4.3.6 Global transcription evaluation

For global transcription evaluation experiments, exponentially-growing MCF-7 cells (2×10^5 per well) were seeded in 15 mm glass bottom cell culture dishes with 2 mL of media and were allowed to attach overnight. Cells were incubated in the presence of 10 μM compounds at 37 °C for 4 h. Cells were washed twice with PBS, incubated 60 min in warmed 1 mM 5-ethynyluridine (EU) medium without FBS at 37 °C, washed twice with PBS and then fixed for 30 min with 4% paraformaldehyde in PBS. After being washed with PBS, cells were permeabilized for 15 min in 0.5% Triton X-100, washed twice with PBS, washed twice with 3% BSA. Click reaction was performed in the dark for 30 min in a buffer containing 50 mM Tris-HCl, 1 mM $CuSO_4$, 10 mM ascorbic acid, 0.5μM Alexa Fluor 647-azide (Invitrogen). Cells were washed with PBS, washed twice with 3% BSA, mounted with fluoroshield mounting buffer containing DAPI for nuclei staining (Solarbio, China).

4.3.7 Fluorescence in situ hybridization (FISH)

For fluorescence *in situ* hybridization (FISH) experiments, exponentially-growing MCF-7 cells (2×10^5 per well) were seeded in 15 mm glass bottom cell culture dishes with 2 mL of media and were allowed to attach overnight. Cells were incubated in the presence of 10 μM compounds at 37 °C for 3 h. Cells

were washed twice with PBS and then fixed for 30 min with 4% paraformaldehyde in PBS. After being washed with PBS, cells were permeabilized for 18 h in 70% ethanol at 4 °C. After two washes with 2 × SSC containing 10% formamide, hybridization was performed in the dark at 37 °C for 5 h in a buffer containing 10% formamide, 2 × SSC, 0.5 mg/mL tRNA, 10% dextran sulfate, 250 mg/mL BSA, 10 mM ribonucleoside vanadyl complexes and 0.5 ng/mL of each probe. Precursors to the 18S rRNA were localized with the 5'-ETS probe (5'-agacgacaacgcctgacacgcacggcac-3') conjugated to Cy5 (localized between the 5'-end of the ETS1 and the 01/A' cleavage site), or with the 5.8S-ITS2 probe (5'-gcgattgatcggcaagcgacgctc-3') conjugated to Cy3 (a probe complementary to the 3'-end of the 5.8S rRNA and the 5'-end of the ITS2) [13, 42]. After two washes at 37 °C with 2 × SSC containing 10% formamide, and mounted with fluoroshield mounting buffer containing DAPI for nuclei staining (Solarbio, China).

4.3.8 Quantitative real-time reverse transcription PCR (qRT-PCR)

MCF-7, A549 and A549cisR cells were plated in 6-well plates at a density of 1 × 10^6 cells/well, respectively, after overnight incubation, the cells were untreated or treated with 10 μM compounds for 3 h. Total RNA was isolated by RNAiso Plus reagent (Takara). RNA was reverse transcribed using the PrimeScript RT reagent Kit (Takara). Quantitative real-time PCR was performed to measure 45S pre-rDNA transcript level using the SYBR Premix Ex Taq™ II Kit (Takara) in CFX96 Real-Time system. The human Actin B RNA was amplified in parallel as the internal control for normalization purpose. The specific primers used are as follows: 45S pre-rRNA (forward) 5'-GCCTTCTCTAGCGATCTGAGAG-3' (reverse) 5'-CCATAACGGAGGCAGAGACA-3', Actin B (forward) 5'-CCTGGCACCCAGCACAAT-3' (reverse) 5'- GGGCCGGACTCGTCATAC-3'. Relative cDNA amounts were estimated using the Ct method [12].

4.3.9 Immunofluorescence (IF)

For immunofluorescence (IF) experiments, exponentially-growing MCF-7 cells (2×10^5 per well) were seeded in 15 mm glass bottom cell culture dishes with 2 mL of media and were allowed to attach overnight. Cells were incubated in the presence of 10 μM compounds at 37 °C for 4 h. Cells were washed twice with PBS and then fixed for 30 min with 4% paraformaldehyde in PBS. After being washed with PBS, cells were permeabilized for 15 min in 0.5% Triton X-100, washed twice with PBS, blocked for 60 min with 1% BSA in PBS, and incubated 120 min with 1:50-1:200 dilution of antibody in 3% BSA. Then cells washed three times for 5 min with PBS; incubated for 30 min with 1:200 dilution of Alexa Fluor 488 labeled secondary antibody (green); washed three times for 5 min with PBS; and mounted with fluoroshield mounting buffer containing DAPI for nuclei staining (Solarbio, China).

4.3.10 Protein extraction, quantification, SDS PAGE and Western Blotting

MCF-7 cells were plated in 6-well plates at a density of 1×10^6 cells/well. After overnight incubation, the cells were treated with different concentrations of compounds and further incubated for 12 h. After that, the cells were collected by trypsinization, washed with cold PBS. Proteins were extracted from the treated cells or the control dish with 100 μL of RIPA buffer containing 1% PMSF, and centrifuged at 12,000 rpm at 4 °C for 2 min. The supernatants were collected as whole cell extracts and stored at −20 °C. Protein concentration was determined by BCA protein assay kit (Solarbio, China). 40 μg of total proteins and color-mixed protein marker (11-180 kD) (Solarbio, China) were separated on 10% sodium dodecyl sulfate-containing polyacrylamide gel and followed by transferring onto polyvinylidene fluoride (PVDF) membranes (EMD, Millipore, USA). The membranes were blocked in TBST (Tris buffered saline with 0.1% Tween-20) containing 5% nonfat milk, and probed with primary antibodies at 4 °C overnight. After the incubation, the membranes were washed with TBST, further incubated with secondary antibody conjugated with horseradish peroxidase, and extensively washed. Finally the results were recorded by Tannon-5200 Multi Image Analyzer (Tannon, China).

4.3.11 Cell cycle arrest assay

MCF-7 cells were plated in 6-well plates at a density of 1×10^6 cells/well, after overnight incubation, the cells were treated with different concentrations of compounds and further incubated for 48 h. After that, the cells were collected by trypsinization, washed with cold PBS, and fixed with 70% ethanol overnight at 4 °C. Before flowcytometric measurements, cells were resuspended and stained by a propidium iodide (PI) staining solution (50 μg/mL PI, 100 μg/mL RNase A) for 15 min at room temperature. Cell cycle distribution was analyzed by a BD Accuri C6 flow cytometer with excitation at 488 nm and emission at 632/15 nm. The data were analyzed by Modifit 3.1 software.

4.3.12 Apoptosis measurements

MCF-7 cells were plated in 6-well plates at a density of 2×10^5 cells/well, after overnight incubation, the cells were treated with different concentrations of compounds and further incubated for 24 h. After that, the cells were collected by trypsinization (without EDTA), washed with cold PBS. Annexin V binding solution (250 μL) was added, then, Annexin V (5 μL of stock solution) and PI solution (2.5 μL of stock solution) were added to the cell suspension for staining according to manufacturer's instructions. After 15 min incubation at room temperature, the samples were analyzed by a BD FACSVerse flow cytometer. The data were analyzed by FlowJo 7.6 software.

4.3.13 Statistical analysis

Unless otherwise stated, all data were expressed as mean ± standard deviation. Statistical significance ($P < 0.05$) was performed by one-way ANOVA followed by an assessment of differences using SPSS 16.0 software.

Notes

The authors declare no competing financial interest.

Acknowledgements

We thank the National Natural Science Foundation of China (No.21371135, No.21401141) and the Tianjin Municipal Nature Science Foundation (No.17JCZDJC33100, No.17JCYBJC28500) for funding support.

References

[1] T.C. Johnstone, K. Suntharalingam, S.J. Lippard, The Next Generation of Platinum Drugs: Targeted Pt(II) Agents, Nanoparticle Delivery, and Pt(IV) Prodrugs, Chem. Rev., 116 (2016) 3436-3486.

[2] A.J. Pickard, U. Bierbach, The cell's nucleolus: an emerging target for chemotherapeutic intervention, ChemMedChem, 8 (2013) 1441-1449.

[3] C. Holohan, S. Van Schaeybroeck, D.B. Longley, P.G. Johnston, Cancer drug resistance: an evolving paradigm, Nat. Rev. Cancer, 13 (2013) 714-726.

[4] M. Dobbelstein, U. Moll, Targeting tumour-supportive cellular machineries in anticancer drug development, Nat. Rev. Drug Discov., 13 (2014) 179-196.

[5] D. Drygin, W.G. Rice, I. Grummt, The RNA polymerase I transcription machinery: an emerging target for the treatment of cancer, Annu. Rev. Pharmacol. Toxicol., 50 (2010) 131-156.

[6] N. Hein, K.M. Hannan, A.J. George, E. Sanij, R.D. Hannan, The nucleolus: an emerging target for cancer therapy, Trends Mol. Med., 19 (2013) 643-654.

[7] L. Montanaro, D. Trere, M. Derenzini, The emerging role of RNA polymerase I transcription machinery in human malignancy: a clinical perspective, Onco. Targets Ther., 6 (2013) 909-916.

[8] M.J. Bywater, G. Poortinga, E. Sanij, N. Hein, A. Peck, C. Cullinane, M. Wall, L. Cluse, D. Drygin, K. Anderes, N. Huser, C. Proffitt, J. Bliesath, M. Haddach, M.K. Schwaebe, D.M. Ryckman, W.G. Rice, C. Schmitt, S.W. Lowe, R.W.

Johnstone, R.B. Pearson, G.A. McArthur, R.D. Hannan, Inhibition of RNA polymerase I as a therapeutic strategy to promote cancer-specific activation of p53, Cancer cell, 22 (2012) 51-65.

[9] D. Drygin, A. Lin, J. Bliesath, C.B. Ho, S.E. O'Brien, C. Proffitt, M. Omori, M. Haddach, M.K. Schwaebe, A. Siddiqui-Jain, N. Streiner, J.E. Quin, E. Sanij, M.J. Bywater, R.D. Hannan, D. Ryckman, K. Anderes, W.G. Rice, Targeting RNA polymerase I with an oral small molecule CX-5461 inhibits ribosomal RNA synthesis and solid tumor growth, Cancer Res., 71 (2011) 1418-1430.

[10] S.J. Woods, K.M. Hannan, R.B. Pearson, R.D. Hannan, The nucleolus as a fundamental regulator of the p53 response and a new target for cancer therapy, Biochim. Biophys. Acta, 1849 (2015) 821-829.

[11] M. Haddach, M.K. Schwaebe, J. Michaux, J. Nagasawa, S.E. O'Brien, J.P. Whitten, F. Pierre, P. Kerdoncuff, L. Darjania, R. Stansfield, D. Drygin, K. Anderes, C. Proffitt, J. Bliesath, A. Siddiqui-Jain, M. Omori, N. Huser, W.G. Rice, D.M. Ryckman, Discovery of CX-5461, the First Direct and Selective Inhibitor of RNA Polymerase I, for Cancer Therapeutics, ACS Med. Chem. Lett., 3 (2012) 602-606.

[12] H. Xu, M. Di Antonio, S. McKinney, V. Mathew, B. Ho, N.J. O'Neil, N.D. Santos, J. Silvester, V. Wei, J. Garcia, F. Kabeer, D. Lai, P. Soriano, J. Banath, D.S. Chiu, D. Yap, D.D. Le, F.B. Ye, A. Zhang, K. Thu, J. Soong, S.C. Lin, A.H. Tsai, T. Osako, T. Algara, D.N. Saunders, J. Wong, J. Xian, M.B. Bally, J.D. Brenton, G.W. Brown, S.P. Shah, D. Cescon, T.W. Mak, C. Caldas, P.C. Stirling, P. Hieter, S. Balasubramanian, S. Aparicio, CX-5461 is a DNA G-quadruplex stabilizer with selective lethality in BRCA1/2 deficient tumours, Nat. Commun., 8 (2017) 14432.

[13] D. Drygin, A. Siddiqui-Jain, S. O'Brien, M. Schwaebe, A. Lin, J. Bliesath, C.B. Ho, C. Proffitt, K. Trent, J.P. Whitten, J.K. Lim, D. Von Hoff, K. Anderes, W.G. Rice, Anticancer activity of CX-3543: a direct inhibitor of rRNA biogenesis, Cancer Res., 69 (2009) 7653-7661.

[14] L. Colis, G. Ernst, S. Sanders, H. Liu, P. Sirajuddin, K. Peltonen, M. DePasquale, J.C. Barrow, M. Laiho, Design, synthesis, and structure-activity relationships of pyridoquinazolinecarboxamides as RNA polymerase I inhibitors, J. Med. Chem., 57 (2014) 4950-4961.

[15] L. Colis, K. Peltonen, P. Sirajuddin, H. Liu, S. Sanders, G. Ernst, J.C. Barrow, M. Laiho, DNA intercalator BMH-21 inhibits RNA polymerase I independent of DNA damage response, Oncotarget, 5 (2014) 4361-4369.

[16] K. Peltonen, L. Colis, H. Liu, R. Trivedi, M.S. Moubarek, H.M. Moore, B. Bai, M.A. Rudek, C.J. Bieberich, M. Laiho, A targeting modality for destruction of RNA polymerase I that possesses anticancer activity, Cancer cell, 25 (2014) 77-90.

[17] S. Ding, X. Qiao, J. Suryadi, G.S. Marrs, G.L. Kucera, U. Bierbach, Using fluorescent post-labeling to probe the subcellular localization of DNA-targeted platinum anticancer agents, Angew. Chem. Int. Ed. Engl., 52 (2013) 3350-3354.

[18] J. Lefebvre, C. Guetta, F. Poyer, F. Mahuteau-Betzer, M.P. Teulade-Fichou, Copper-Alkyne Complexation Responsible for the Nucleolar Localization of Quadruplex Nucleic Acid Drugs Labeled by Click Reactions, Angew. Chem. Int. Ed. Engl., 56 (2017) 11365-11369.

[19] C.P. Montgomery, B.S. Murray, E.J. New, R. Pal, D. Parker, Cell-penetrating metal complex optical probes: targeted and responsive systems based on lanthanide luminescence, Acc. Chem. Res., 42 (2009) 925-937.

[20] K. Singh, S. Singh, P. Srivastava, S. Sivakumar, A.K. Patra, Lanthanoplatins: emissive Eu(iii) and Tb(iii) complexes staining nucleoli targeted through Pt-DNA crosslinking, Chem. Commun., 53 (2017) 6144-6147.

[21] L.E. Wedlock, M.R. Kilburn, R. Liu, J.A. Shaw, S.J. Berners-Price, N.P. Farrell, NanoSIMS multi-element imaging reveals internalisation and nucleolar targeting for a highly-charged polynuclear platinum compound, Chem. Commun., 49 (2013) 6944-6946.

[22] M. Tsekrekou, K. Stratigi, G. Chatzinikolaou, The Nucleolus: In Genome

Maintenance and Repair, Int. J. Mol. Sci., 18 (2017) 1411.

[23] P.M. Bruno, Y. Liu, G.Y. Park, J. Murai, C.E. Koch, T.J. Eisen, J.R. Pritchard, Y. Pommier, S.J. Lippard, M.T. Hemann, A subset of platinum-containing chemotherapeutic agents kills cells by inducing ribosome biogenesis stress, Nat. Med., 23 (2017) 461-471.

[24] E.J. Peterson, V.R. Menon, L. Gatti, R. Kipping, D. Dewasinghe, P. Perego, L.F. Povirk, N.P. Farrell, Nucleolar targeting by platinum: p53-independent apoptosis follows rRNA inhibition, cell-cycle arrest, and DNA compaction, Mol. Pharm., 12 (2015) 287-297.

[25] X. Qiao, S. Ding, F. Liu, G.L. Kucera, U. Bierbach, Investigating the cellular fate of a DNA-targeted platinum-based anticancer agent by orthogonal double-click chemistry, J. Biol. Inorg. Chem., 19 (2014) 415-426.

[26] K. Peltonen, L. Colis, H. Liu, S. Jaamaa, Z. Zhang, T. Af Hallstrom, H.M. Moore, P. Sirajuddin, M. Laiho, Small molecule BMH-compounds that inhibit RNA polymerase I and cause nucleolar stress, Mol. Cancer Ther., 13 (2014) 2537-2546.

[27] Z. Ma, L. Rao, U. Bierbach, Replacement of a thiourea-S with an amidine-NH donor group in a platinum-acridine antitumor compound reduces the metal's reactivity with cysteine sulfur, J. Med. Chem., 52 (2009) 3424-3427.

[28] L.A. Graham, G.M. Wilson, T.K. West, C.S. Day, G.L. Kucera, U. Bierbach, Unusual Reactivity of a Potent Platinum-Acridine Hybrid Antitumor Agent, ACS Med. Chem. Lett., 2 (2011) 687.

[29] S. Ding, X. Qiao, G.L. Kucera, U. Bierbach, Using a Build-and-Click Approach for Producing Structural and Functional Diversity in DNA-Targeted Hybrid Anticancer Agents, J. Med. Chem., 55 (2012) 10198.

[30] J. Suryadi, U. Bierbach, DNA metalating-intercalating hybrid agents for the treatment of chemoresistant cancers, Chem. Eur. J., 18 (2012) 12926-12934.

[31] A.J. Pickard, F. Liu, T.F. Bartenstein, L.G. Haines, K.E. Levine, G.L. Kucera, U. Bierbach, Redesigning the DNA-Targeted Chromophore in Platinum-Acridine

Anticancer Agents: A Structure-Activity Relationship Study, Chem. Eur. J., 20 (2014) 16174-16187.

[32] T.A. Connors, M.J. Cleare, K.R. Harrap, Structure-activity relationships of the antitumor platinum coordination complexes, Cancer Treat. Rep., 63 (1979) 1499-1502.

[33] A. Ghezzi, M. Aceto, C. Cassino, E. Gabano, D. Osella, Uptake of antitumor platinum(II)-complexes by cancer cells, assayed by inductively coupled plasma mass spectrometry (ICP-MS), J. Inorg. Biochem., 98 (2004) 73-78.

[34] X. Qiao, A.E. Zeitany, M.W. Wright, A.S. Essader, K.E. Levine, G.L. Kucera, U. Bierbach, Analysis of the DNA damage produced by a platinum-acridine antitumor agent and its effects in NCI-H460 lung cancer cells, Metallomics, 4 (2012) 645-652.

[35] M.U. Khan, P.J. Sadler, Distribution of a platinum anti-tumour drug in HeLa cells by analytical electron microscopy, Chem. Biol. Interact., 21 (1978) 227-232.

[36] M. Horky, G. Wurzer, V. Kotala, M. Anton, B. Vojtesek, J. Vacha, J. Wesierska-Gadek, Segregation of nucleolar components coincides with caspase-3 activation in cisplatin-treated HeLa cells, J. Cell Sci., 114 (2001) 663-670.

[37] P. Jordan, M. Carmo-Fonseca, Cisplatin inhibits synthesis of ribosomal RNA in vivo, Nucleic Acids Res., 26 (1998) 2831-2836.

[38] N. Vlatkovic, M.T. Boyd, C.P. Rubbi, Nucleolar control of p53: a cellular Achilles' heel and a target for cancer therapy, Cell. Mol. Life Sci., 71 (2014) 771-791.

[39] T. Ozdian, D. Holub, Z. Maceckova, L. Varanasi, G. Rylova, J. Rehulka, J. Vaclavkova, H. Slavik, P. Moudry, P. Znojek, J. Stankova, J.B. de Sanctis, M. Hajduch, P. Dzubak, Proteomic profiling reveals DNA damage, nucleolar and ribosomal stress are the main responses to oxaliplatin treatment in cancer cells, J. Proteomics, 162 (2017) 73-85.

[40] S. Ding, X. Qiao, G.L. Kucera, U. Bierbach, Design of a

platinum-acridine-endoxifen conjugate targeted at hormone-dependent breast cancer, Chem. Commun, 49 (2013) 2415-2417.

[41] Y.M. Liang, X. Wang, R. Ramalingam, K.Y. So, Y.W. Lam, Z.F. Li, Novel nucleolar isolation method reveals rapid response of human nucleolar proteomes to serum stimulation, J. Proteomics, 77 (2012) 521-530.

[42] C. Carron, M.F. O'Donohue, V. Choesmel, M. Faubladier, P.E. Gleizes, Analysis of two human pre-ribosomal factors, bystin and hTsr1, highlights differences in evolution of ribosome biogenesis between yeast and mammals, Nucleic Acids Res., 39 (2011) 280-291.

Highlights

- A novel monofunctional platinum Pol I-selective inhibitor **P1-B1** has been reported.
- **P1-B1** displays significant nucleolar accumulation.
- **P1-B1** selectively inhibits Pol I transcription machinery.
- **P1-B1** induces nucleolar stress, cell cycle arrest and apoptosis.
- **P1-B1** is mechanistically distinct from the effects of conventional platinum agents.